ARCHIVES OF ELECTRICAL ENGINEERING VOL. 63(4), pp. 609-619 (2014)

DOI 10.2478/aee-2014-0042

Modeling of a two stages electrostatic air precipitation process using response surface modeling

DJELLOUL BERRACHED, AMAR TILMATINE, FARID MILOUA, MALIKA BENGRIT

APELEC Laboratory, Djillali Liabes University
Sidi Bel-Abbes, Algeria
e-mail: atilmatine@gmail.com

(Received: 14.07.2014, revised: 17.09.2014)

Abstract: Any industrial process needs to work with the optimal operating conditions and thus the evaluation of their robustness is a critical issue. A modeling of a laboratory-scale wire-to-plane two stages electrostatic precipitator for guiding the identification of the set point, is presented this in paper. The procedure consists of formulating recommendations regarding the choice of optimal values for electrostatic precipitation. A two-stages laboratory precipitator was used to carry out the experiments, with samples of wood particles of average granulometric size 10 µm. The parameters considered in the present study are the negative applied high voltage of the ionization stage, the positive voltage of the collection stage and the air speed. First, three "one-factor-at-a-time" experiments were performed followed by a factorial composite design experiments, based on a two-step strategy: 1) identify the domain of variation of the variables; 2) set point identification and optimization of the process.

Key words: electrostatic precipitator, two-stage ESP, design of experiments, experimental modeling

1. Introduction

Electrostatic precipitation is an effective way to remove solid particulate pollutants (such as dust and smoke) or liquid (fog, oil, mist) contained in the gas injected into the environment [1-4]. This precipitation process is one of the numerous applications of high voltage [5-8] and is now widely used in apartments, offices and hospitals, as well as workshops, because of its low power consumption and high precipitation efficiencies (up to 99.9%) [9-10]. Besides the huge electrostatic precipitators (ESP) that purify the flue gases of cement plants, foundries or thermal power stations, many smaller size units have been developed for the treatment of ambient air in workshops, offices, hospitals and the like, at very low electric energy consumption and high particle retention efficiency [11-12].

In spite of several studies published on these issues in recent years [13-17], no standard procedure is available for guiding the research of the set point and for identifying the factors

that should be better controlled for the process to be claimed robust. The difficulty of the problem resides in the fact that electrostatic precipitation is a multifactorial process. In a "wire-to-plane" ESP comprising an ionizing and a collecting stages, for instance, the list of factors influencing the efficiency of the process includes the voltage levels of both stages, the pollution rate, the granule size, the electrode configuration, the air speed and so on...

The aim of the present paper is the identification of the process set point using an experimental procedure based on the response surface modeling, which is succefuly used in other case-studies such as the electrostatic separators of particles [18-21]. The work of this paper was carried out for the choice of the high-voltage level of both ionization and collection stages, and the air speed. Three one-factor-at-a-time experiments corresponding to each factor, followed by a composite factorial design, were performed based on the following two-step strategy: 1) Identify the domain of variation of the variables; 2) Set point identification and optimization of the process.

2. Experimental designs methodology

Before starting the experiments, it is necessary to set the best and suitable design which can model the process with the most possible precision [22-24]. In this paper, the Composite Centred Faces design (CCF), which gives quadratic models, was adopted. It is possible to determine a quadratic dependence between the output function to optimize (response) and the input variables u_i ($i = 1, ..., k$) (factors):

$$y = f(u_i) = c_0 + \sum c_i u_i + \sum c_{ij} u_i u_j + \sum c_{ii} u_i^2. \tag{1}$$

Knowing that Δu_i and u_{i0} are respectively the step of variation and the central value of factor i, reduced centred values of input factors may be defined by the following relation:

$$x_i = \frac{(u_i - u_{i0})}{\Delta u_i}. \tag{2}$$

With these new variables, the output function becomes:

$$y = f(x_i) = a_0 + \sum a_i x_i + \sum a_{ij} x_i x_j + \sum a_{ii} x_i^2. \tag{3}$$

The coefficients can be calculated or estimated by a data-processing program, in such a way to have a minimum variance between the predictive mathematical model and the experimental results.

MODDE 5.0 software (Umetrics AB, Umea, Sweden) was used, which is a Windows program for the creation and the evaluation of experimental designs [25]. The program assists the user for interpretation of the results and prediction of the responses. It calculates the coefficients of the mathematical model and identifies best adjustments of the factors for optimizing the process. Moreover, the program calculates two significant statistical criteria which make it possible to validate or not the mathematical model, symbolized by R^2 and Q^2. The former is

called the goodness of fit, and is a measure of how well the model can be made to fit the raw data; it varies between 0 and 1, where 1 indicates a perfect model and 0 no model at all. The latter is called goodness of prediction, and estimates the predictive power of the model. Like R^2, Q^2 has the upper bound 1, but its lower limit is minus infinity. For a model to pass the diagnostic test, both parameters should be high, and preferably not separated by more than 0.2-0.3.

3. The experimental set-up and methods

The tests were performed on a laboratory electrostatic precipitator, configured as in Figure 1. The experimental bench is composed of 2 stages (Fig. 2): first the polluting particles pass through the ionization stage where they are electrically charged by corona discharge and then are collected in the collection stage by an intense electrostatic field generated between parallel plate electrodes (aluminum, 300×200 mm). The ionization stage comprises 4 units, each consisting of three vertical wires (tungsten, diameter 0.1 mm), energized from a negative high-voltage supply (ISEG, 60 kV, 9 mA), and equally distant from vertical plate electrodes (aluminum, 300×20 mm) connected to the ground. The inter-electrode gap of the ionization stage is d = 3 cm and for the collection stage D = 2 cm.

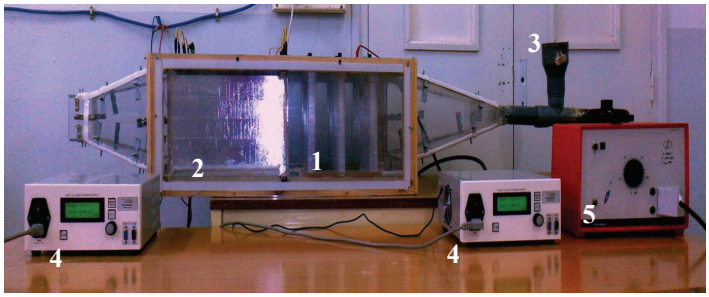

Fig. 1. The laboratory experimental device: 1) ionization stage; 2) collection stage; 3) input of wood particles; 4) high voltage supplies; 5) AC variable supply of the blower

Wood particles of average granulometric size 10 μm were used as pollutant material. The dust was prepared using vibrating sieves and the particles of average diameter 10 μm were used as pollutant material. Therefore, the overall average diameter was uniform, while the density being equal to 1.4 g/dm^3.

The circulation of the polluted air is performed by means of an air blower of 1.45 kW with a maximal rotation speed of 1280 rev/min, the flow rate being adjusted using an AC variable voltage source.

The efficiency is calculated using following relation

$$\eta(\%) = \frac{m_i - m_s}{m_s} \times 100. \tag{4}$$

Where: m_i – total mass of wood articles introduced into ESP, m_s – not filtered mass recovered at the exit of the clean gas.

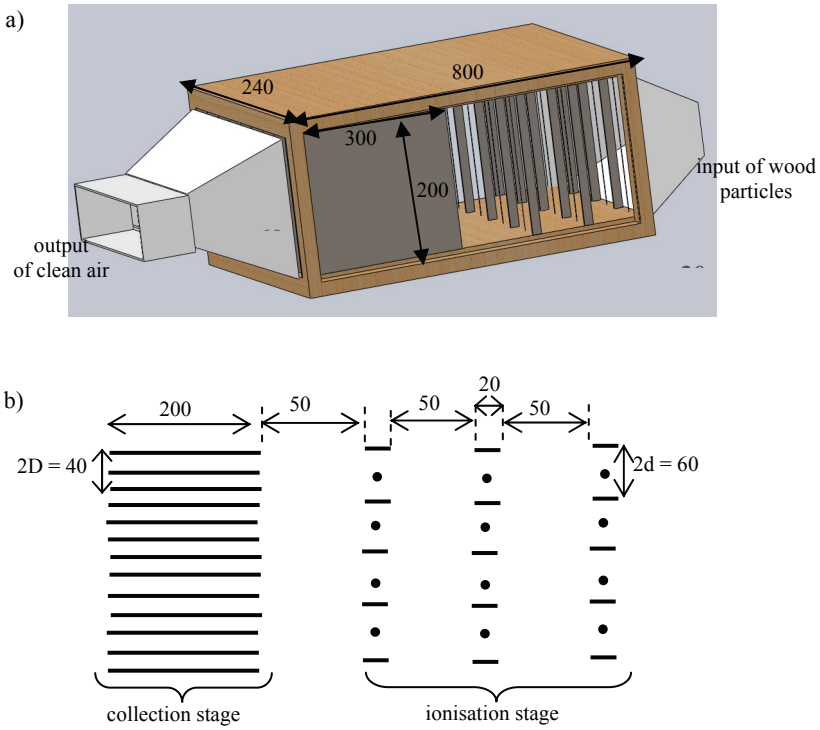

Fig. 2. Descriptive representation of the two stages ESP a) overall 3D view, b) schematic description (all dimensions are in mm)

The mass was measured using digital balance of resolution 0.1 g. All tests were carried out under stable environmental conditions: 18-20°C, 40-50 RH%.

Three factors were considered in the present stusy:

- the ionization voltage *Vi* (kV);
- the collection voltage *Vc* (kV);
- the air speed *n*(m/s).

To measure the dust mass at the outlet of the ESP, an air filter was fixed at the exit of the particles in order to recover the non filtered particles.

An experimental procedure of two steps was adopted:

Step 1. Define domain of variation of the factors (Vi_{min} and Vi_{max}, Vc_{min} and Vc_{max}, v_{min} and v_{max}) with three experiments "one-factor-at-a-time":

Experiment 1.1. Voltage *Vi* variable (8 to 16) kV, with constant voltage *Vc* = 15 kV and air speed *n* = 6 m/s.

Experiment 1.2. Voltage *Vc* variable (11 to 23) kV, with constant voltage *Vi* = 12 kV and air speed *n* = 6 m/s.

Experiment 1.3. Air speed *n* variable (5 to 7 m/s), with constant voltage *Vi* = 12 kV and voltage *Vc* = 15 kV.

Step 2. Define set-point operation by performing a composite centered faces design CCF.

4. Results and discussion

Step 1. Variation domain of factors.

For more precision, all experiments in this work were done twice and the average value was used for plotting. These data were used for definition of the variation domain of *Vi*, *Vc* and n for Step 2 of the experimental procedure. Results of Experiments 1.1 are illustrated in Figure 3.

Thus, the graph in Figure 3 shows that in the conditions of Experiment 1.1, describing the variation of the precipitation efficiency as function of the ionization voltage *Vi*, the efficiency is increasing with voltage *Vi* up to 16 kV. Beyond this value, the corona discharge generated by the ionizing electrodes stops due to the breakdown of air occurring when *Vi* is higher than 16 kV. Thus, V_{min} = 13 kV and V_{max} = 16 kV were selected as the limit values of the variation domain for *Vi*.

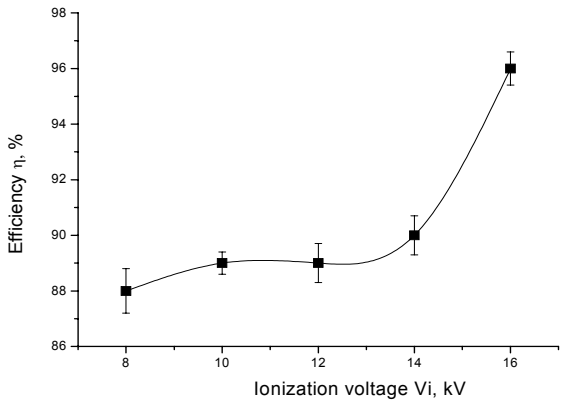

Fig. 3. Variation of the precipitation efficiency according to ionization voltage

The variation of the efficiency process according to the collection voltage *Vc* shown in Figure 4 points out that the efficiency increases up to 14 kV and then decreases to 17 kV to finally increase up to 24 kV. The decrease was caused by a second "unwanted" corona discharge occurring on the edges of the collecting electrodes. To avoid this problem, the electrodes were rearranged in such a way to increase the gap distance between adjacent electrodes (Fig. 5). A second variation curve was obtained with the new configuration of the electrodes (Fig. 6), from which minimal and maximal values of *Vc* were determined as follows: $V_{c\,min}$ = 13 kV and $V_{c\,max}$ = 16 kV.

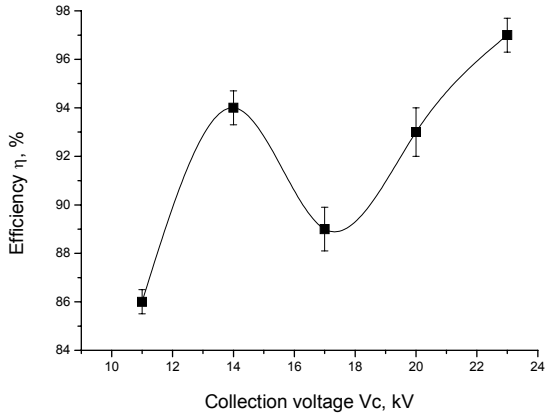

Fig. 4. Variation of the precipitation efficiency according to collection voltage *Vc*

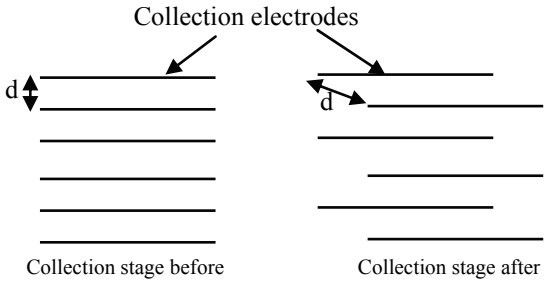

Fig. 5. Position of the collecting electrodes to avoid the "unwanted" corona discharge

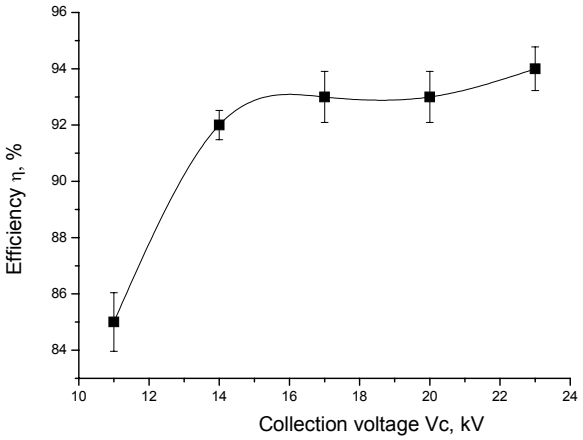

Fig. 6. Variation of the precipitation efficiency according to the collection voltage (for the new configuration of the collecting electrodes)

Obtained results in Figure 7 show that the precipitation efficiency of the process decreases with the air speed due to the increase of the aerodynamic force $\boldsymbol{F_a}$ which acts almost perpendicullary to the electric force $\boldsymbol{F_e}$. Thus, the variation domain of air speed n was delimited by $n_{\min} = 5.6$ m/s and $n_{\max} = 6.4$ m/s.

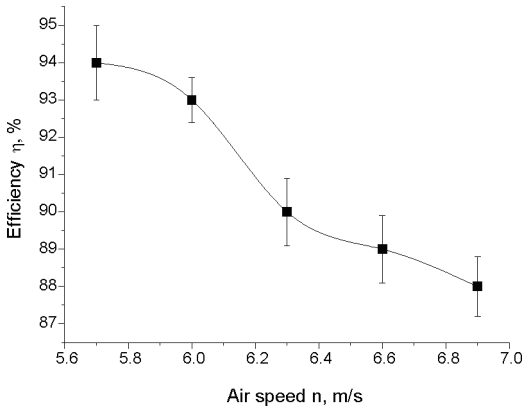

Fig. 7. Variation of the precipitation efficiency according to the air speed

Step 2. Set point identification

Design of experiments methodology is useful for screening, optimization and robustness testing. Screening experiments were designed in this paper to identify the domain of variation of the three factors. The optimization stage of an experimental procedure should enable the determination of factor values for which the precipitation efficiency is a maximum.

The identification of the set point (Vi_0, Vc_0 and n_0) by using a central CCF design was performed; the two levels "max" and "min" are the limits established in previous section for each of the three control variables, ($Vi_{\min}$, $Vi_{\max}$), ($Vc_{\min}$, $Vc_{\max}$) and ($n_{\min}$, $n_{\max}$), and, the central point (Vi_0, V_{c0} and n_0) being calculated as follows:

$$V_{i0} = \frac{(Vi_{\min} + Vi_{\max})}{2} = \frac{13+16}{2} = 14.5 \text{ kV}, \tag{5}$$

$$V_{c0} = \frac{(Vc_{\min} + Vc_{\max})}{2} = \frac{13+16}{2} = 14.5 \text{ kV}, \tag{6}$$

$$V_0 = \frac{(V_{\min} + V_{\max})}{2} = \frac{5.6+6.4}{2} = 6 \frac{\text{m}}{\text{s}}, \tag{7}$$

The results of the CCF experimental design are given in Table 1.

The mathematical model of the response considered for optimization, which is the precipitation efficiency, was obtained with MODDE 5.0 as follows

$$y = 96.4 + 1.42Vi^* - 0.58Vc^* + 0.36n^* - 1.44Vi^{*2} - 1.05Vc^{*2} +$$

$$+ 1.45n^{*2} - 0.48Vi^*Vc^* - 0.16Vc^*n^*.$$

The two statistical criteria computed by MODDE 5.0 were quite satisfactory (i.e., close to unity) for both models: the goodness of fit $R^2 = 0.97$; the goodness of prediction $Q^2 = 0.84$. Figure 8 represents the coefficients of the model as plotted by MODDE.05.

Table 1. Results of the CCF experimental design

Exp N°	**Voltage *Vi* (kV)**	**Voltage *Vc* (kV)**	**Air speed *n* (m/s)**	**Efficiency (%)**
1	13.0	13.0	5.6	93.2
2	16.0	13.0	5.6	97.5
3	13.0	16.0	5.6	93.9
4	16.0	16.0	5.6	95.3
5	13.0	13.0	6.4	94.8
6	16.0	13.0	6.4	98.0
7	13.0	16.0	6.4	93.9
8	16.0	16.0	6.4	96.1
9	13.0	14.5	6.0	93.6
10	16.0	14.5	6.0	96.7
11	14.5	13.0	6.0	96.3
12	14.5	16.0	6.0	94.8
13	14.5	14.5	5.6	97.7
14	14.5	14.5	6.4	98.4
15	14.5	14.5	6.0	96.2
16	14.5	14.5	6.0	95.7
17	14.5	14.5	6.0	96.7

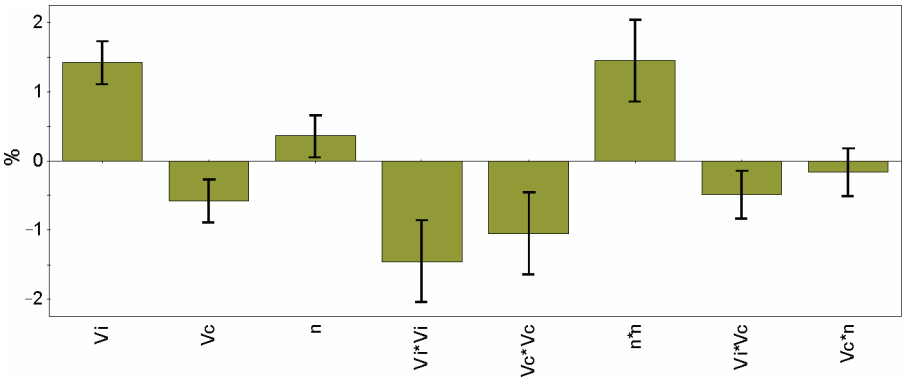

Fig. 8. Coefficients of the model plotted by MODDE.05

The coefficients of the proposed mathematical model represent the degree of influence of all factors and interactions between them. Therefore, a high value of the coefficient means that the factor which affects the coefficient is significant, and vice versa. Voltage *Vi* has the most

important effect on the precipitation efficiency, the corresponding coefficient in the regression model being 1.42, due to the enhancement of the particle charging when the electric field is increased. The increase of voltage *Vc*, which is unfortunately accompanied by an augmentation of the corona current in the collection stage, causes a decrease of the efficiency. In addition, we noticed any significant interaction between the three factors.

Iteration: 5002 Iteration slider:

	1	2	3	4	5	6
	Ionization voltage	Collection voltage	Air speed	Efficiency	iter	log(D)
1	15,1613	14,3002	6,4	98,6921	1032	-10
2	15,3187	13,9979	5,6	97,9735	5000	0,2657
3	15,3157	14,0246	5,6	97,9735	5001	0,2656
4	15,1744	14,2481	6,4	98,7162	742	-10
5	15,4312	14,2067	6,4	98,7262	861	-10

Response	Criteria	Weight	Min	Target	Max
Efficiency	Maximiz	1	98,1474	98,6334	

Fig. 9. Results of the optimization routine of MODDE 5.0 for maximization of the precipitation efficiency

According to this model, the optimum of the process corresponding to the highest value of the precipitation efficiency should be obtained for *Vi* = 15.1 kV, *Vc* = 14.3 kV and *n* = 6.4 m/ (Fig. 9). "iter" is the number of iterations and Log(D) is the Log of overall distance to the target; the value of Log(D) equals zero when all responses are between Target and Limit. The smaller Log(D), the better is the result. Log(D) becomes negative when the values of all responses are still closer to the Target [25].

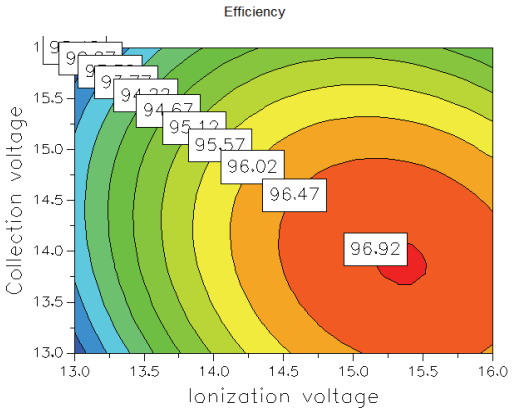

Fig. 10. Response contour plots of the response for *n* = 6 m/s

Even though it is commonly known that the air flow increases the particle drag and reduces the precipitation efficiency, according to obtained results, the collection efficiency at 6.4 m/s (row 1) is higher than that for 5.6 m/s (second row). It's established in ESP process that particles collection is mainly performed at the input of the ESP especially when the par-

ticles velocity is lower. Thus, the efficiency is better when a greater collection surface is concerned which happens when the velocity is slightly higher.

Figure 10 shows the iso-response contours obtained with the present model, describing the dependency of the precipitation efficiency according to the variation of both ionization and collection voltages. According to this figure, it follows that voltage *Vi* is indeed more influent in the electrostatic precipitation process. The efficiency is maximal when *Vi* lies between 15.1 kV and 15.5 kV and *Vc* between 13.2 kV and 14.5 kV.

5. Conclusions

The electrostatic precipitation using ionization and collections stages is a multi factors process and thus needs to be optimized regarding to the most influent parameters. In this paper, three factors were analyzed: the ionization voltage, the collection voltage and the air speed. A set-point corresponding to the optimal values of these factors was identified using response surface modeling, which gives the maximal precipitation efficiency.

References

[1] Jedrusik M., Swierczok A., Teisseyre R., *Experimental study of fly ash precipitation in a model electrostatic precipitator with discharge electrodes of different design.* Powder Technology: 295-301 (2003).
[2] Hoenig, S.A., *New application of electrostatic technology to control of dust, fumes, smokes and aerosols*. IEEE Transactions on Industry Applications IAS-17(4): 386-391 (1981).
[3] White HJ., *Industrial Electrostatic Precipitation, Reading, MA.* Wesley G.O. (1963).
[4] Onda K., Kasuga Y., Kato K. et al., *Electric discharge removal of $SO_2$and NO_2 from combustion flue gas by pulsed corona discharge.* Energy Conversion and Management 38: 1377-1387 (1997).
[5] Balcerak M., Hołub M., Pałka R., *High voltage pulse generation using magnetic pulse compression.* Archives of Electrical Engineering 62(3): 463-472 (2013).
[6] Hołub M., *Study on the influence of output inductance on DBD plasma uniformity.* Archives of Electrical Engineering 63(2): 263-272 (2014).
[7] Balcerak M., Hołub M., Pałka R., *High voltage pulse generation using magnetic pulse compression.* Archives of Electrical Engineering 62(3): 463-472 (2013).
[8] Masłowski G., *Corona current concept in lightning return-stroke models of engineering type*. Archives of Electrical Engineering 59(3-4): 177-188 (2010).
[9] Artino A., Cârdu M., *Electrostatic precipitators used in the ecological conversion of power in coal-fired thermoelectric power plants.* Energy Convers Manage 35: 477-81 (1994).
[10] Macarie R., Martin D., *New technologies for the electrostatic precipitators pulsed energization in energetic.* Energy Convers Manage 38: 511-6 (1997).
[11] Miloua, F., Gouri, R., Tilmatine, A. et al., *Optimization of the rapping pro-cess of an intermittent electrostatic precipitator.* European Physical Journal of Applied Physics, EDP Sciences 41(1): 81-85 (2008).
[12] Remaoun SM., Tilmatine A., Miloua F. et al., *Optimization of a Cost-Effective"Wire-Plate"Type ESP for Installation in a Medical Wastes Incinerator.* IEEE/IAS Joint. Conference on Electrostatics, Waterloo, Canada, pp. 12-15 (2012).
[13] Adamiak K., *Numerical models in simulating wire-plate electrostatic precipitators: a review*. J. Electrostatics 71: 673-80 (2013).

[14] Khalid U., Eldein A., *Experimental study of V-Icharacteristics of wire-plate electrostatic precipitators under clean air conditions*. J. Electrostatics 71: 228-34 (2013).
[15] Gajewski J.B., *Accuracy of cross correlation velocity measurements in two-phase gasesolidflows.* Flow Meas. Instrum 30: 133-137 (2013).
[16] Juliusz B., Gajewski., *Monitoring of electrostaticfire and explosion hazards at the inlet to electrostatic precipitators.* Journal of Electrostatics 72: 192-197 (2014).
[17] Al-Hamouz Z., *Numerical and experimental evaluation of fly ash collection efficiency in electrostatic precipitators*. Energy Conversion and Management 79: 487-497 (2014).
[18] Miloudi M., Medles K., Tilmatine A. et al., *Modeling and optimization of a propeller-type tribocharger for granular materials*. Journal of Electrostatics 69(6): 631-637 (2011).
[19] Rezouga M., Tilmatine A., Ouiddir R., Medles K, *Experimental Modelling of the Breakdown Voltage of Air Using Design of Experiments Advances in electrical and computer engineering.* Acadamy of Technical Science of Romania 9(1): 41-45 (2009).
[20] Medles K., Tilmatine A., Rezouga M. et al., E*xperimental Designs Methodology And Its Application to an Electrostatic Separation Process.* Materials Technology: Advanced Performance Materials 21(3): 144-147(4) (2006).
[21] Medles K., Dascalescu L., Tilmatine A. et al., *Experimental Modeling of the Electrostatic Separation of Granular Materials.* Particulate Science and Technology, http://www.informaworld.com/smpp/title~content=t713774907~db=all~tab=issueslist~branches=25 - v2525 (2): 163-171, (2007).
[22] Frigon N.L., Mathews D., *Practical Guide to Experimental Design.* 1st ed., Wiley, New York (1996).
[23] Taguchi G., *System of Experimental Designs*. Kraus International Publications, New York (1987).
[24] Eriksson L., Johansson E., Kettaneh-Wold N. et al., *Design of Experiments, Principles and Applications*. Learnways AB, Stockholm (2000).
[25] MODDE 5.0, *User guide and tutorial*. Umetrics (1999).